

Electromigration-Induced Flow of Islands and Voids on the Cu(001) Surface

Hanoch Mehl, Ofer Biham and Oded Millo

Racah Institute of Physics, The Hebrew University, Jerusalem 91904, Israel

Majid Karimi

Physics Department, Indiana University of Pennsylvania, Indiana, PA 15705

Electromigration-induced flow of islands and voids on the Cu(001) surface is studied at the atomic scale. The basic drift mechanisms are identified using a complete set of energy barriers for adatom hopping on the Cu(001) surface, combined with kinetic Monte Carlo simulations. The energy barriers are calculated by the embedded atom method, and parameterized using a simple model. The dependence of the flow on the temperature, the size of the clusters, and the strength of the applied field is obtained. For both islands and voids it is found that edge diffusion is the dominant mass-transport mechanism. The rate limiting steps are identified. For both islands and voids they involve detachment of atoms from corners into the adjacent edge. The energy barriers for these moves are found to be in good agreement with the activation energy for island/void drift obtained from Arrhenius analysis of the simulation results. The relevance of the results to other FCC(001) metal surfaces and their experimental implications are discussed.

I. INTRODUCTION

Electromigration (EM) describes the biased diffusion processes of bulk and surface atoms under the influence of an applied electric field [1–3]. The driving force is composed of two major components: one is the direct electrostatic interaction between the applied field and the conductor ions and the second, denoted as the “wind force” is due to momentum transfer from the conduction electrons impinging upon the ionic cores. The EM force F is characterized by an effective charge Z^* of the ions, which quantifies its strength according to $F = eZ^*E$, where E is the electric field. In metals, the wind force is the dominant component, thus Z^* is negative [2,4]. The problem of EM in metal films has been extensively investigated experimentally and theoretically for over three decades [5–8]. The interest in this problem was motivated by the fact that EM has been identified as a major failure mode of metal interconnects in microelectronic devices, where current densities as large as 10^6 A/cm², are typical [9,10]. Indeed, significant experimental effort was directed at material and technological issues, aimed to reduce EM-induced damage. These issues include the choice of metal to be used (e.g. Al, AlCu alloys, or Cu

dominated alloys), deposition procedures and wire geometries.

Statistical properties of EM phenomena have been studied extensively as a function of applied current density and temperature. These properties include the time to failure of metal wires under current stress [2,5,11], drift velocities [12,13], resistance-noise [14], as well as resistance increase rates [3,11,15,16]. Experimental results were analyzed using phenomenological equations, such as the Black equation [5], that relates the mean time to failure t_{mean} to a *single* activation energy Q through $t_{mean} \propto j^{-2} \exp(Q/k_B T)$, where j is the current density and T is the temperature. A similar equation is also used to analyze the resistance-increase rate [3,17,18]. This approach provides a useful characterization of the wire performance and reliability. However, it does not yield much insight into the fundamental processes that give rise to EM. Particularly, the assumption that there is only one activation energy is inadequate. This is manifested in the dispersion of activation energies reported in the literature for a given material. Taking Cu as an important example, we find a broad range of reliably measured activation energies, e.g., 0.47 eV [15], 0.7-0.9 eV [12], 0.79 eV [17] and 1.21 eV [11]. These results indicate that EM is not driven by a single atomic diffusion process, but is a complex phenomenon that involves a wide spectrum of activation energies, and depends on the microscopic details of the samples.

A large variety of EM-related phenomena have been observed, such as thinning, void (and hillock) formation, followed by their growth and migration [2,3]. The rate at which each of these processes develops depends on the dominant atomic diffusion mechanism involved. In particular, one can distinguish between atom diffusion inside crystallites, along grain boundaries, and diffusion on surfaces and interfaces. Grain boundary diffusion is believed to be dominant in polycrystalline materials [2,3]. However, surface (and interface) diffusion becomes more important as the cross section of the wire decreases. Hence, studies of surface EM at the atomic and nanometer scales may provide much insight into the fundamental EM-induced processes. Recent studies of surface EM on single crystal Si samples have focused on EM-induced step dynamics [19–21]. The mobility of steps and dislocations in thin polycrystalline metal films has also been studied [22,23]. In theoretical studies using a continuum description, the effects of EM on atomic steps [24] and

voids [25,26] were examined.

In this paper we present a detailed study of diffusion of single islands and voids of monoatomic height on the Cu(001) surface, under electromigration conditions. In our analysis we employ a complete set of hopping energy barriers for Cu atoms on the Cu(001) surface, obtained using the embedded atom method (EAM) [27]. The biased diffusion of islands and voids is studied using energy considerations and kinetic Monte-Carlo (MC) simulations. The different mechanisms involved in the diffusion of islands and voids are identified and the activation energies of the corresponding rate-limiting steps are quantified. The drift velocities are obtained as a function of the EM bias, island/void size and the surface temperature. For both islands and voids the slopes of the Arrhenius plots obtained from the simulation results are found to be in excellent agreement with the activation energies of the rate-limiting steps, and thus confirm their identification. The drift velocities are found to be linear with the bias magnitude.

The paper is organized as follows. In Sec. II we present the model and assumptions. The relevant atomic processes are presented in Sec. III. The simulations and results are shown in Sec. IV, followed by a discussion and summary in Sec. V.

II. MODEL AND ASSUMPTIONS

Surface diffusion is described by thermally activated hopping processes of adatoms. The hopping rate h (in units of hops per second) of a given atom to each unoccupied nearest neighbor (NN) site is given by

$$h = \nu \cdot \exp(-E_B/k_B T) \quad (1)$$

where $\nu = 10^{12} \text{ s}^{-1}$ is the commonly used attempt rate, E_B is the activation energy barrier, k_B is the Boltzmann constant and T is the temperature.

The activation energy barrier E_B depends on the local environment of the hopping atom, namely the configuration of occupied and unoccupied adjacent sites. We assume that only nearest and next-nearest neighbor sites have a non-negligible effect on the activation energy. On FCC(001) surfaces, under these assumptions, the hopping energy barrier is determined by the occupation of seven adjacent sites, as shown in Fig. 1. In this model, adatoms diffuse along the principal crystal directions. On the FCC(001) surface, the possible paths are along the $x = \langle 011 \rangle$ and $y = \langle 0\bar{1}1 \rangle$ axes.

In the simulations described below we use a set of energy barriers for Cu on Cu(001) [28,29], which includes all possible local environments of the hopping atom. The effect of the electric current is incorporated by lowering the barrier for diffusion in the direction of the electron flow, and by raising it in the opposite direction. Thus, if the barrier for a certain process is E_B without bias, it will be $E_B - \Delta$ for that process in the direction of

the bias, and $E_B + \Delta$ in the opposite direction. The bias Δ is proportional to the applied field according to $\Delta = eZ^*E \cdot a$, where a is the projection of the hopping distance along the bias direction. In this paper we focus on the case in which the field is parallel to either the x or the y axis. Thus, for Cu, $a = 2.55 \text{ \AA}$, which is the lattice constant of the resulting two dimensional square lattice. We also assume that bias Δ is the same for all processes and barriers. Although the distortion in the energy landscape may depend on the local configuration, no details are known about this dependence. It is also assumed that the dependence of the attempt frequency ν on the field is weak enough, and can be neglected.

Consider a single object (adatom, dimer, vacancy etc.) diffusing on the Cu(001) surface. The net drift of this object in the x direction after time t , will be: $\Delta x = n_+ - n_-$, where n_+ and n_- are the numbers of hops in the positive and negative directions of the x axis respectively. On time scales much longer than the time for a single hop, the average number of hops will be proportional to the elapsed time and to the hopping rate. Assume now that the bias is in the positive x direction. According to the model we have:

$$\langle n_{\pm} \rangle = t\nu \cdot e^{-\frac{E_B \mp \Delta}{k_B T}}, \quad (2)$$

thus the average drift velocity in the x direction will be:

$$\langle v \rangle = \frac{\langle x \rangle}{t} = 2h \cdot \sinh\left(\frac{\Delta}{k_B T}\right), \quad (3)$$

where $h = \nu \cdot \exp(-E_B/k_B T)$ is the rate of the hopping process without any bias [Eq. (1)]. The drift velocity of a given object is proportional to its hopping rate, namely, it depends exponentially on the activation energy, just like the diffusion coefficient. The proportionality factor, $\sinh(\Delta/k_B T)$, is common to all processes, and depends on the temperature and the applied field. Under physically relevant condition $\Delta \ll k_B T$ (see below). Therefore $\sinh(\Delta/k_B T)$ can be approximated by $\Delta/k_B T$, and the drift velocity is linearly proportional to the bias.

III. ATOMIC DESCRIPTION OF CLUSTER DRIFT

A. The Energy Barriers

Within the assumptions described above, adatom diffusion on the Cu(001) surface involves $2^7 = 128$ hopping processes (Fig. 1). In order to obtain the rates of these processes one needs to calculate their energy barriers. Our analysis is based on semi-empirical calculations obtained via the embedded atom method (EAM) [27]. This method provides a good description of self diffusion of Cu on Cu(001) [28], as well as self diffusion on other metal surfaces [30,31]. Specifically, we use the EAM functions of Cu developed by Adams, Foiles, and

Wolfer [32] which are fitted to a similar data base as the one employed by Foiles, Baskes, and Daw [33]. Generally, these energy barriers are in agreement with those obtained using other semi-empirical methods such as the effective medium theory (EMT) [34,35], and ab-initio calculations [36]. Though each process has a different activation energy, they can be roughly divided into four groups [29,37]. These groups give rise to four typical time scales in the problem which span over several orders of magnitude. These time scales correspond (in ascending order) to attachment processes, edge diffusion, free surface hopping and detachment processes. We will argue that all four scales are essential in the description of cluster drift. Furthermore, even much smaller differences between processes which belong to the same group will appear to be significant.

B. Simple Model for Energy Barriers

The calculated energy barriers can be well approximated by a simple model which has four parameters [29]. This model provides a systematic description of the energetics of the hopping processes, and a classification of these processes to four groups. It also enables generalization to different materials. According to the model, the energy barrier E_B for a certain process depends on the seven sites of Fig. 1 as follows:

$$E_B = E_0 + E_{NN}^{in} \cdot (S_3 + S_1 + S_5) - E_{NN}^{top} \cdot (S_1 + S_5 + S_2 + S_6) + E_{NNN} \cdot (S_0 + S_2 + S_4 + S_6) \quad (4)$$

where $S_i = 1$ if site i is occupied and $S_i = 0$ if it is vacant, E_0 is the barrier for an isolated adatom hopping on the surface, E_{NN}^{in} and E_{NNN} are the effective binding energies of the hopping atom to its nearest and next-nearest neighbors, respectively. The highest energy along the hopping path is obtained in the vicinity of the bridge site. The binding energy of the hopping adatom at this highest point, to an atom in one of the four adjacent sites is given by E_{NN}^{top} . Here we use a simplified version of the model assuming that $E_{NN}^{in} \simeq E_{NN}^{top}$. This approximate degeneracy is found for most FCC metals [29,37]. The expression we use for the barriers is thus

$$E_B^n = E_0 + E_{NN} \cdot (S_3 - S_2 - S_6) + E_{NNN} \cdot (S_0 + S_2 + S_4 + S_6). \quad (5)$$

The three parameters E_0 , E_{NN} and E_{NNN} were estimated for Cu(001) and yielded $E_0 = 0.49$ eV, $E_{NN} = 0.27$ eV and $E_{NNN} = 0.027$ eV [29,37]. While simple and intuitive, the barriers obtained from the model may deviate in some cases significantly from the EAM barriers. Such deviations occur in relatively dense local environments, where several sites in both sides of the hopping atom are occupied. The model accounts for the complex

interactions between these atoms only on the average. In the following discussion barriers obtained by both EAM and the model of Eq. (5) are quoted. The data for the simulation results presented below were obtained using the EAM barriers.

C. Physical Conditions

The following discussion concentrates on clusters of 60-1000 atoms/vacancies on the Cu(001) surface. Such clusters are typically created during deposition and sputtering experiments [38,39]. We consider temperatures in the range 200-600K, which is the relevant range for most experimental studies. The model for diffusion described above applies well in this regime, where no other hopping mechanisms are significant. At higher temperatures additional processes may take place [36].

The effective charge for EM in bulk copper was found experimentally to be $Z^* \approx -5$ [1]. For surface EM there exist only theoretical estimations. These calculations found the effective charge to be of the same order of magnitude, $Z^* \approx -20$ [4,40], almost independent of surface orientation and diffusion path. Typical current densities in EM experiments (and in integrated circuits) are $j \approx 10^6 - 10^7$ A/cm². The resistivity of Cu under typical conditions is $\rho \approx 2 \cdot 10^{-6}$ Ω·cm. If we assume that the current is distributed uniformly across the conductor's cross-section, we find the EM force acting on surface atom to be $F = eZ^*j\rho \approx 10$ eV/cm. For Cu(001) the distance between adjacent sites is ≈ 2.55 Å. The work done by the EM force during one hop in the bias direction is thus $\approx 10^{-7}$ eV. Intuitively, this would be the change in the energy barrier for the process. Since most of the relevant barriers are in the range 0.1-0.8 eV, we find that Δ is typically 6-7 orders of magnitude smaller than E_B . For such a small bias to produce any effect an extremely long time is required. In experiments, it takes at least several hours at temperatures higher than 400°C for any significant change. Simulating systems at these temperatures for more than a second is beyond the power of contemporary computers. To overcome this difficulty, we use bias values in the range $\Delta \approx 10^{-3} - 10^{-4}$ eV. These values are larger than the realistic ones, but still much smaller (2-3 orders of magnitude) than the diffusion barriers. The linear response approximation is thus still valid.

D. Island Drift

During the drift, clusters (islands and voids) maintain an approximate square shape with small fluctuations and rounded corners. There is experimental evidence that this is the equilibrium shape of islands [38,39]. These experiments show that even if a different shape is created (during coalescence, for example), it rearranges to

the square-like pattern within several minutes at room temperature. This is a consequence of the square symmetry of the lattice and the fast edge diffusion. This fact has important implication on the atomic details of island diffusion, with or without bias. When clusters diffuse, they typically move one lattice site at a time, while maintaining their equilibrium shape in the new position. Although the bias drives the system out of equilibrium, since the applied bias is small, the basic pattern is preserved. This feature is also observed in our computer simulations. However, in the presence of bias, atoms drift along island edges with a preferable direction, and thus sharpen the rounded corners in the bias direction. The basic cycle of island drift, in which the center of mass moves one lattice site in the bias direction, can be divided to three main stages. These are shown schematically in Fig. 2. To describe the basic cycle, take the starting point to be an island with a straight edge in the direction of the drift. [Fig. 2(a)]. First, an atom detaches from one of the four corners and arrives at the island front [Fig. 2(b)]. Next, several other atoms nucleate to this atom from the corners and create a new row of atoms in the front [Fig. 2(c)]. Last, atoms from the rear side of the island fill the place of the atoms that formed the new row and straighten the corners to form a configuration similar to that of Fig. 2(a), shifted by one lattice site in the bias direction. The entire process can now repeat as the drift goes on. We will now go into the details of each stage.

Consider an island with a straight front edge in the drift direction as in Fig. 2(a). One atom now detaches from one of the corners and arrives at this front. If it detached from a rear corner (with respect to the drift direction), it will hop along the sides parallel to the drift under the bias influence, and arrive at the front. There are four possible moves in which an atom can leave the corners, which we index from (a) to (d), as shown in Figs. 3(a-d), respectively. All these processes actually take place, but we will now argue that one of them is much more probable, and thus determines the properties of the drift. This process is an escape from a straight corner [Fig. 3(a)]. By escape here we mean the detachment of an atom from a relatively bound configuration to the island edge, but not a complete detachment from the island.

The activation energy for this move is given by:

$$\begin{aligned} E_{\text{escape}}(a) &= E_0 + E_{NN} + E_{NNN} \\ &= 0.79\text{eV}(\text{model}), 0.78\text{ eV (EAM)}, \end{aligned} \quad (6)$$

where the first number corresponds to the model [Eq. (5)], and the second number is the EAM barrier. After the first of the two hops which compose the move in Fig. 3(a) has taken place, there are even chances (neglecting the bias) for that atom to go back to the corner or to actually escape to the straight edge. Another possibility is the escape from a straight edge [Fig. 3(b)]. The barrier for such event is

$$\begin{aligned} E_{\text{escape}}(b) &= E_0 + E_{NN} + 2E_{NNN} \\ &= 0.82\text{eV}(\text{model}), 0.90\text{ eV (EAM)}. \end{aligned} \quad (7)$$

It may seem at first sight that the extra NNN bond in comparison to the corner escape may be compensated by the large number of atoms at this configuration along the island edges. This is not the case, however, because an actual escape can happen only one lattice position off the corners, and not anywhere along the edges. Otherwise, the escaped atom is most likely to return to its initial position. Furthermore, as mentioned before, the barriers obtained by the model are less accurate at dense environments. The corresponding EAM barrier for the escape from straight edge is 0.9 eV. Another possibility is the escape from a rounded (kinked) corner [Fig. 3(c)]. The expression obtained from the model for this barrier is the same as in Eq. (7). The EAM barrier for this move is $E_{\text{escape}}(c) = 0.83\text{ eV}$, which is slightly higher than that for move (a). Also, at this configuration several other processes are much more likely to happen before an escape move takes place. The last move (d) is an escape of an atom from an edge kink followed by hopping around a corner [Fig. 3(d)]. The barrier for each of these processes separately (E_k and E_c respectively) is lower relative to the previous three:

$$\begin{aligned} E_k &= E_0 + 2E_{NNN} \\ &= 0.54\text{ eV}(\text{model}), 0.48\text{ eV(EAM)}, \end{aligned} \quad (8)$$

and

$$\begin{aligned} E_c &= E_0 + E_{NNN} \\ &= 0.52\text{ eV}(\text{model}), 0.54\text{ eV(EAM)}, \end{aligned} \quad (9)$$

To understand why this move is relatively unlikely, it should be noticed that in most cases the atom will re-attach to the kink rather than hop around the corner. The barrier for a move from the corner back towards the kink site is low: $E_{\text{back}} = E_0 - E_{NN} + E_{NNN} [=0.24\text{ eV}(\text{model}), 0.18\text{ eV(EAM)}]$. The average number of times the atom has to detach from the kink until it hops once around the corner is given by

$$(h_c + h_{\text{back}})/h_c \simeq \exp[(E_c - E_{\text{back}})/k_B T], \quad (10)$$

since $h_c \ll h_{\text{back}}$ for the relevant temperature range. The prefactor depends on the distance between the kink and the corner. The effective barrier for the move shown in Fig. 3(d) is

$$\begin{aligned} E_{\text{escape}}(d) &= E_k + E_c - E_{\text{back}} \\ &= E_0 + E_{NN} + 2E_{NNN} \\ &= 0.82\text{eV}(\text{model}), 0.84\text{ eV (EAM)}. \end{aligned} \quad (11)$$

The next stage in the island drift process is the nucleation of other atoms to the atom hopping along the straight facet. The basic mechanism for this nucleation is shown in Fig. 4. The energy barrier for this process is

$$\begin{aligned}
E_{nuc} &= E_0 + 3E_{NNN} \\
&= 0.57 \text{ eV(model)}, 0.53 \text{ eV(EAM)},
\end{aligned} \tag{12}$$

This process must occur several times in order to create a stable new row of atoms on the existing facet. Still, the time scale of this nucleation process is short compared to that of the escape process. The ratio between the rates of these processes is at least

$$\begin{aligned}
&\exp[(E_{escape} - E_{nuc})/k_B T] \simeq \\
&\simeq \exp[(E_{NN} - 2E_{NNN})/k_B T].
\end{aligned} \tag{13}$$

For Cu, this ratio is 125 at 600 K and more than 15000 at room temperature. In the clusters we consider, where a typical linear island size is of 10-30 atoms, this is a relatively fast process.

Now, atoms from the edges parallel to the bias direction will fill-in the kinks created by the atoms that moved to the new row. This stage is necessary to enable the nucleation of the next new row. This is due to the high rate of adatom re-attachment to kinks. There are two basic mechanisms for this edge drift which are shown in Fig. 5. In Fig. 5(a) a single atom hops along the edge in the bias direction. Eventually this atom will be absorbed in a kink site at the island corner. In Fig. 5(b) the same happens with an edge vacancy in the opposite direction. The barriers for these processes are

$$\begin{aligned}
E_a &= E_0 - E_{NN} + 2E_{NNN} \\
&= 0.27 \text{ eV(model)}, 0.25 \text{ eV(EAM)},
\end{aligned} \tag{14}$$

and

$$\begin{aligned}
E_b &= E_0 + 2E_{NNN} \\
&= 0.54 \text{ eV(model)}, 0.48 \text{ eV(EAM)},
\end{aligned} \tag{15}$$

The first one is of course much faster, but requires an escape move to begin with. To estimate the time scale of these processes, one needs to obtain the average number of single hopping events required for one atom/vacancy that leaves one corner to be absorbed at the opposite one. It is reasonable to treat both atoms and vacancies as one dimensional random walkers. The problem then reduces to a random walk with two absorbing barriers. The expression obtained from the theory of biased random walks (see e.g. Ref. [41]), depends on the bias and the length of the walk (i.e. the linear size of the island). In the range of these two parameters we deal with, the results are 26-200 events. Again, this is a short time scale compared to that of escape events. In summary, the drift of islands can be divided into three stages with three different time scales. The velocity of the drift is determined by the slowest of these, namely the escape event. We come to the conclusion that the escape process (a) is the rate limiting step of island drift. The effective barrier for the drift is thus

$$\begin{aligned}
E_B(\text{island drift}) &= E_{escape}(a) \\
&= E_0 + E_{NN} + E_{NNN} \\
&= 0.79 \text{ eV(model)}, 0.78 \text{ eV (EAM)}.
\end{aligned} \tag{16}$$

E. Void Drift

Basically, the three stages that exist in the island drift process, are found for vacancy clusters as well. The atomic details however, reveal important differences. The most essential difference is in the equivalent process to the corner escape move. Consider a void with a straight corner (Fig. 6). The barrier for this detachment process is

$$\begin{aligned}
E_{detach} &= E_0 + 3E_{NNN} \\
&= 0.57 \text{ eV(model)}, 0.53 \text{ eV(EAM)}.
\end{aligned} \tag{17}$$

In most cases however, the detached atom does not escape from the corner, but goes back to its initial position. There are several possible moves in the nearby environment that may prevent the detached atom from moving back. The one with the lowest barrier is the replacement move shown in Fig. 6. The average number of times a detachment event should occur before such move takes place, is very well approximated by the ratio of the rates

$$h_{back}/h_{replace} = \exp[(E_{replace} - E_{back})/k_B T]. \tag{18}$$

The effective barrier obtained for an escape from the corner is

$$\begin{aligned}
E_{escape} &= E_{detach} + E_{replace} - E_{back} \\
&= E_0 + E_{NN} + 3E_{NNN} \\
&= 0.84 \text{ eV(model)}, 0.73 \text{ eV (EAM)}.
\end{aligned} \tag{19}$$

The nucleation of other vacancies on the void edge is created mainly by the detachment of atoms from an edge kink and their diffusion along the edge (Fig. 7). The bottleneck of this process is the move across the corner of the void, shown in Fig. 7(b). The barrier for leaving the corner is $E_c = E_0 + 3E_{NNN}$ [=0.57 eV(model), 0.53 eV(EAM)].

$$\begin{aligned}
E_c &= E_0 + 3E_{NNN} \\
&= 0.57 \text{ eV(model)}, 0.53 \text{ eV(EAM)},
\end{aligned} \tag{20}$$

In contrast to islands, void corners are “attractive”. Since the barrier for leaving the corner is comparable to the barrier for leaving edge kink, in many cases there will be no accumulation of atoms near the corner, and we will not get the rounded corners as in islands. In other words, the stages of nucleation and corner straightening are combined in voids. In order to compare the time scales of the stages, we need to estimate how many corner detachment events are required for one atom to reach the opposite edge of the void. (The hopping on the edge itself is again very fast and its actual time is negligible.) Using again the approximation of a one dimensional random walk, we obtain an estimation of ≈ 10 such events for voids of linear size 10. Since all atoms on the facet must go through the corner, at least 100 events are required for the nucleation of a complete row. The time

scale of the nucleation stage is thus short compared to that of the escape event at low temperatures. Under these conditions the effective barrier for void drift is

$$E_B(\text{void drift}) = E_{\text{escape}} = E_0 + E_{NN} + 3E_{NNN} \\ = 0.84\text{eV}(\text{model}), 0.73\text{ eV (EAM)}. \quad (21)$$

At higher temperatures, however, depending on the size of the cluster and the bias, the two time scales may become comparable.

F. The Drift Velocity

For both islands and voids we identified the rate limiting processes and their energy barriers. These barriers are the effective activation energies of the entire drift process. We thus expect the drift velocities of islands and voids to scale like

$$v_{\text{drift}}(\text{island}) \sim \exp\left(-\frac{E_0 + E_{NN} + E_{NNN}}{k_B T}\right) \quad (22)$$

and

$$v_{\text{drift}}(\text{void}) \sim \exp\left(-\frac{E_0 + E_{NN} + 3E_{NNN}}{k_B T}\right) \quad (23)$$

respectively. It is convenient to measure the velocity of the cluster center of mass in units of lattice sites per second. We expect from Eq. (3) that the drift velocity is linearly proportional to the bias magnitude. It is also proportional to the probability of an escaped atom to form a new row rather than go back. This probability cannot be deduced from simple arguments, since it generally involves a random walk with moving boundaries and many particles. In general it may depend on the cluster size and the temperature. For larger clusters, more atoms need to nucleate to complete a new front row. It also takes longer to fill the kink site created by each newly nucleated atom, since the sides parallel to the bias component are now longer. We thus expect that the prefactor decreases as the cluster size increases, but cannot provide a specific functional form.

IV. SIMULATIONS AND RESULTS

In the simulations reported below we used the continuous time kinetic MC technique [42–48]. This technique is particularly suitable for the simulation of non-equilibrium processes, keeping track of the physical time in a realistic manner. During the kinetic MC simulation, the next move is selected randomly from the list of all possible moves at the given time with the appropriate weights. The time is advanced after each move according to the inverse of the sum of all rates. All the processes allowed by the model are incorporated in the simulations with the appropriate energy barriers. In the simulation

results presented below we used barriers for Cu/Cu(001) obtained by EAM [29].

We have performed systematic simulations on single isolated islands and voids. The initial island and void configurations were chosen to be of a square shape from the reasons already discussed. The morphology and location of the clusters were followed for different temperatures, bias directions, and bias magnitudes. This was repeated for different sizes of the islands/voids. As expected, islands drift in the direction of the bias, while vacancy clusters drift in the opposite direction. In the temperature range considered here (200 – 500K), both islands and voids drift as a whole, since the activation energy for a complete detachment of atoms or vacancies is high relative to the processes discussed above. Furthermore, even if an atom/vacancy is detached from the cluster, the bias is not strong enough for a substantial drift, and it will re-attach after few moves.

In the simulations we follow the displacement of the center of mass of the clusters as a function of the physical time. It was found that under the EM bias, clusters drift on the average at a constant velocity. The dependence of this velocity on the cluster size, bias magnitude and the temperature is shown below.

A. The Effect of Bias Magnitude on the Drift Velocity.

We found that the drift velocity of islands depends linearly on the bias as can be seen from Fig. 8. This dependence is expected from Eq. (3), and was confirmed by simulations for bias magnitudes in the range $\Delta \approx 10^{-3}$ – 10^{-5} eV. In addition we confirmed by simulations that the effect of bias direction is given by $v_x \propto \Delta \cos(\phi)$ and $v_y \propto \Delta \sin(\phi)$, where v_x and v_y are the x and y components of the drift velocity, and Δ is the bias magnitude applied in an angle ϕ relative to the x axis.

B. Drift Velocity as a Function of the Temperature

The dependence of the drift velocity on the temperature is shown in Fig. 9. The activation energy for island diffusion, is found by the best exponential fit to be $E_B(\text{island drift}) = 0.78 \pm 0.02$ eV. This coincides with the energy barrier for the escape move, which we identified as the rate limiting step in the analysis above. For voids, we find that for temperatures in the range $220\text{K} < T < 300\text{K}$ there is a good fit to the predicted value: $E_B(\text{void drift}) = 0.73 \pm 0.02$. At higher temperatures there is a small deviation from this value towards a lower value. This may indicate that the probability of an atom that escaped from a void corner to be re-attached rather than start a new vacancy row, slightly depends on the temperature.

C. Dependence of The Drift Velocity on Cluster Size

Fig. 10 shows the dependence of the drift velocity on the linear size of the cluster. As could be expected, there is a monotonic decrease in drift velocity. The quantitative details, however, are not completely concluded.

V. DISCUSSION AND SUMMARY

In this paper we have studied the mechanisms of EM-driven diffusion of single islands and voids on the Cu(001) surface. We found that the drift velocity of a cluster of a given linear size depends on the bias Δ and the temperature T according to

$$v(T, \Delta) = A \cdot \frac{\Delta}{k_B T} \nu \cdot \exp(-Q/k_B T), \quad (24)$$

where Q is the activation energy of the rate limiting step of the drift process and A is a constant. The reciprocal dependence on the temperature could not be inspected from the simulation results, since it is much weaker than the exponential dependence. It is deduced, however, from the discussion following Eq. (3), and from dimensional analysis. The activation energy Q is given by Eq. (16) for islands and by Eq. (21) for voids.

The value of the constant A is proportional to the probability of an escaped atom to form solid nucleation and establish a new front row of atoms. As we mentioned before, the atomic diffusion processes that determine this probability are complicated. The simulations, however, yield a value of $A \sim 5 - 20$ for islands, and $A \sim 40 - 80$ for voids, depending on the cluster size, provided that the velocity is measured in units of lattice sites per second.

It was found [37] that most FCC(001) metal surfaces share the same qualitative features of the different hopping mechanisms. The hopping energy barriers in these systems can be parameterized by models similar to the one we used here, with the specific parameters appropriate for each metal. The analysis of the atomic processes involved in the drift of islands and voids, and their typical time scales should be thus valid for these FCC(001) metal surfaces as well. Several simulations performed for Ag/Ag(001) diffusion, indicate that this is indeed the case.

Extrapolation of the results to other regimes are reasonable as long as the relations between the time scales remain as in the above discussion. Larger clusters or weaker bias may be considered as long as the nucleation and corner straightening stages are still faster relative to the escape move. For islands at room temperatures, for example, this means clusters of up to $\sim 10^4$ atoms at bias of 0.001 eV, or bias down to $\sim 10^{-6}$ eV for clusters of ~ 100 atoms. The linear dependence of the drift velocity on the bias makes the extrapolation down to a more realistic bias values straightforward.

In order to test our predictions experimentally one needs to prepare Cu(001) surfaces with islands of the desired size distribution. Then one needs to drive current along the surface at high current densities. Using scanning tunneling microscope (STM) one will be able to measure the drift velocities of different islands and obtain their dependence on the island size, bias and temperature. Related experimental work has been done on diffusion of islands on Cu(001) with no bias [38] and the dependence of the diffusion coefficient on island size was obtained. To our knowledge, no such experiments on single crystal metal surfaces have been done under EM conditions. It seems that a serious difficulty in performing such experiments on single crystal samples may be to reach the high current densities required to obtain a fast enough drift, due to the considerable width of such samples.

ACKNOWLEDGMENTS

We thank J. Krug for helpful discussions. We would like to acknowledge support from the Intel-Israel college relations committee during the initial stages of this work, and from the Israeli Ministry of Science and Technology during the final stages.

-
- [1] H. B. Huntington, *Diffusion in Solids* (Academic, New-York, 1975), p. 303.
- [2] P.S. Ho and T. Kwok, Rep. Prog. Phys. **52**, 301 (1989).
- [3] R.W. Vook, Mater. Chem. & Phys. **36**, 199 (1994).
- [4] P.J. Rous, T.L. Einstein and E.D. Williams, Surf. Sci. Lett. **315**, L995 (1994).
- [5] J.R. Black, in *Proc. 6th Ann. Intl. Reliab. Phys. Symp.* (1967), p. 148.
- [6] I.A. Blech and E.S. Meiran, Appl. Phys. Lett. **11**, 263 (1967).
- [7] P.S. Ho and H.B. Huntington, J. Phys. Chem. Sol. **27**, 1319 (1966).
- [8] R. Rosenberg and L. Berenbaum, Appl. Phys. Lett. **12**, 201 (1968).
- [9] J.R. Lloyd and J.J. Clement, Thin Solid Films **262**, 135 (1995).
- [10] *Materials Reliability in Microelectronics VI*, edited by W.F. Filter, J.J. Clement, A.S. Oates, R. Rosenberg and P.M. Lenahan (Materials Research Society, Pittsburgh, PA, 1996).
- [11] A. Gladkikh, Y. Lereah, M. Karpovski, A. Palevski, Yu.S. Kaganovskii, in *Materials Reliability in Microelectronics VI*, edited by W.F. Filter, J.J. Clement, A.S. Oates, R. Rosenberg and P.M. Lenahan (Materials Research Society, Pittsburgh, PA, 1996), p. 55.
- [12] C.-K. Hu, K.L. Lee, D. Gupta and P. Blauner, in *Materials Reliability in Microelectronics VI*, edited by W.F. Filter, J.J. Clement, A.S. Oates, R. Rosenberg and P.M. Lenahan (Materials Research Society, Pittsburgh, PA, 1996), p. 43.
- [13] M. Gall, D. Jawarani and H. Kawasaki, in *Materials Reliability in Microelectronics VI*, edited by W.F. Filter, J.J. Clement, A.S. Oates, R. Rosenberg and P.M. Lenahan (Materials Research Society, Pittsburgh, PA, 1996), p. 81.
- [14] K. Dagge, in *Materials Reliability in Microelectronics VI*, edited by W.F. Filter, J.J. Clement, A.S. Oates, R. Rosenberg and P.M. Lenahan (Materials Research Society, Pittsburgh, PA, 1996), p. 147.
- [15] B.H. Jo and R.W. Vook, App. Surf. Sci. **89**, 237 (1995).
- [16] A.H. Verbruggen, et. al., in *Materials Reliability in Microelectronics VI*, edited by W.F. Filter, J.J. Clement, A.S. Oates, R. Rosenberg and P.M. Lenahan (Materials Research Society, Pittsburgh, PA, 1996), p. 121.
- [17] C.W. Park and R.W. Vook, Appl. Phys. Lett. **59**, 175 (1991).
- [18] R.W. Vook and B.H. Jo, in *Materials Reliability in Microelectronics VI*, edited by W.F. Filter, J.J. Clement, A.S. Oates, R. Rosenberg and P.M. Lenahan (Materials Research Society, Pittsburgh, PA, 1996), p. 31.
- [19] E.D. Williams, E. Fu, Y.-N. Yang, D. Kandel and J.D. Weeks, Surf. Sci. **336**, L746 (1995).
- [20] Y.-N. Yang, E.S. Fu and E.D. Williams, Surf. Sci. **356**, 101 (1996).
- [21] E.S. Fu, D.J. Liu, M.D. Johnson and E.D Williams, Surf. Sci. **385**, 259 (1997).
- [22] N. Shimoni, M. Wolovelsky, O. Biham and O. Millo, Surf. Sci. **380**, 100 (1997).
- [23] N. Shimoni, O. Biham and O. Millo, Surf. Sci. **414**, L925 (1998).
- [24] D. Kandel and J.D. Weeks, Phys. Rev. Lett. **74**, 3632 (1995).
- [25] O. Kraft, U.E. Mockl and E. Arzt, in *Materials Reliability in Microelectronics VI*, edited by W.F. Filter, J.J. Clement, A.S. Oates, R. Rosenberg and P.M. Lenahan (Materials Research Society, Pittsburgh, PA, 1996), p. 161.
- [26] M. Schimschak and J. Krug, Phys. Rev. Lett. **80**, 1674 (1998).
- [27] M. S. Daw and M. I. Baskes, Phys. Rev. Lett. **50**, 1285 (1983).
- [28] M. Karimi, T. Tomkowski, G. Vidali and O. Biham, Phys. Rev. B **52**, 5364 (1995).
- [29] O. Biham, I. Furman, M. Karimi, G. Vidali, R. Kennett and H. Zeng, Surf. Sci. **400**, 29 (1998).
- [30] C.-L. Liu, J. M. Cohen, J. B. Adams and A. F. Voter, Surf. Sci. **253**, 334 (1991).
- [31] L. S. Perkins and A. E. DePristo, Surf. Sci. **325**, 169 (1995).
- [32] J. B. Adams, S. M. Foiles and W. G. Wolfer, J. Mater. Res. **4**, 102 (1989).
- [33] S. M. Foiles, M. I. Baskes and M. S. Daw, Phys. Rev. B **33**, 7983 (1986).
- [34] K. W. Jacobsen, J. K. Norskov and M. J. Puska, Phys. Rev. B **35**, 7423 (1987).
- [35] L. Hansen, P. Stoltze, K.W. Jacobsen and J.K. Norskov, Phys. Rev. B **44**, 6523 (1991).
- [36] G. Boisvert and L. J. Lewis, Phys. Rev. B **56**, 7643 (1997).
- [37] H. Mehl, O. Biham, I. Furman and M. Karimi, Models for Adatom Diffusion on FCC(001) Metal Surfaces, Phys. Rev. B, in press (1999).
- [38] W.W. Pai, A.K. Swan, Z. Zhang and J.F. Wendelken, Phys. Rev. Lett. **79**, 3210 (1997).
- [39] C.R. Stoldt, A.M. Cadilhe, C.J. Jenks, J.-M. Wen, J.W. Evans and P.A. Theil, Phys. Rev. Lett. **81**, 2950 (1998).
- [40] P.J. Rous, T.L. Einstein and E.D. Williams, Phys. Rev. B **53**, 13909 (1996).
- [41] S. K. Srinivasan and K. M. Mehata, *Stochastic Processes* (McGraw-Hill, New Delhi, 1976), p. 99.
- [42] A. Bortz, M. Kalos, and J. Lebowitz, J. Chem. Phys. **17**, 10 (1975).
- [43] A.F. Voter, Phys. Rev. B **34**, 6819 (1986).
- [44] K. Fichthorn and W.H. Weinberg, J. Chem. Phys. **95**, 1090 (1991).
- [45] Y.-T. Lu and H. Metiu, Surf. Sci. **245**, 150 (1991).
- [46] S. Clarke, M. R. Wilby and D. D. Vvedensky, Surf. Sci. **255**, 91 (1991).
- [47] H.C. Kang and W.H. Weinberg, Surf. Sci. **299/300**, 755 (1994).
- [48] G. T. Barkema, O. Biham, M. Breeman, D. O. Boerma, and G. Vidali, Surf. Sci. Lett. **306**, L569 (1994).

FIG. 1. Classification of all possible local environments of a hopping atom including seven adjacent sites. Each site can be either occupied or unoccupied, giving rise to $2^7 = 128$ local environments. Sites 1, 3 and 5 are nearest neighbors of the original site while sites 1, 2, 5 and 6 are adjacent to the bridge site that the atom has to pass.

FIG. 2. The main stages in cluster drift starting from a straight facet (a). An atom is detached from the corner and starts a new row (b). Other atoms nucleate to the first atom and complete the row (c). Atoms then drift along the edges and retain the straight facet. The arrow on the grid indicates the initial position of the lattice front.

FIG. 3. The main mechanisms for detachment that starts a new row: (a) from a straight corner, (b) from a kinked corner, (c) from a straight edge and (d) from a kinked edge. It is found that (a) has the lowest activation energy and is thus dominant.

FIG. 4. The main mechanism for nucleation of atoms on a new row. Notice that it can take place only near the corners, and that the inverse process is identical.

FIG. 5. The main mechanisms for atom drift along island edges. (a) A single atom hops on a straight edge; and (b) an edge vacancy drifts in the opposite direction. The arrow indicates the bias direction.

FIG. 6. The atomic process that starts a new vacancy row in a void drift. An atom is detached from the straight corner. Another atom may fill its place and create a stable dimer.

FIG. 7. Nucleation of vacancies at the new vacancy row is actually composed of atom detachment from an edge kink (a), hopping to the corner of the void (b), and then to the opposite corner.

FIG. 8. Drift velocity as a function of bias magnitude for 10×10 clusters. Stars are voids at temperature of 350K and Circles are islands at 400K. Error bars are about the size of the symbols.

FIG. 9. Drift velocity as a function of T^{-1} on semi-logarithmic scale, for 10×10 island (stars) and void (circle) with bias of 0.003 eV. Solid lines are a fit to an exponential form $A \cdot \exp(\frac{-Q}{k_B T})$. The temperature range is 300-400K and the error bars are smaller than the symbols. The slopes obtained from the fit are $Q = 0.78 \pm 2$ eV for islands. For voids at $T < 300$ K $Q = 0.73 \pm 2$ eV. These values are in agreement with the barriers of the rate limiting steps discussed in the text.

FIG. 10. Drift velocity as a function of cluster size for (a) islands at bias of 0.002 eV and (b) voids at bias of 0.0005 eV. The temperature is 400K. The error bars in (a) correspond to one standard deviation of the runs, while in (b) they are smaller than the symbols.

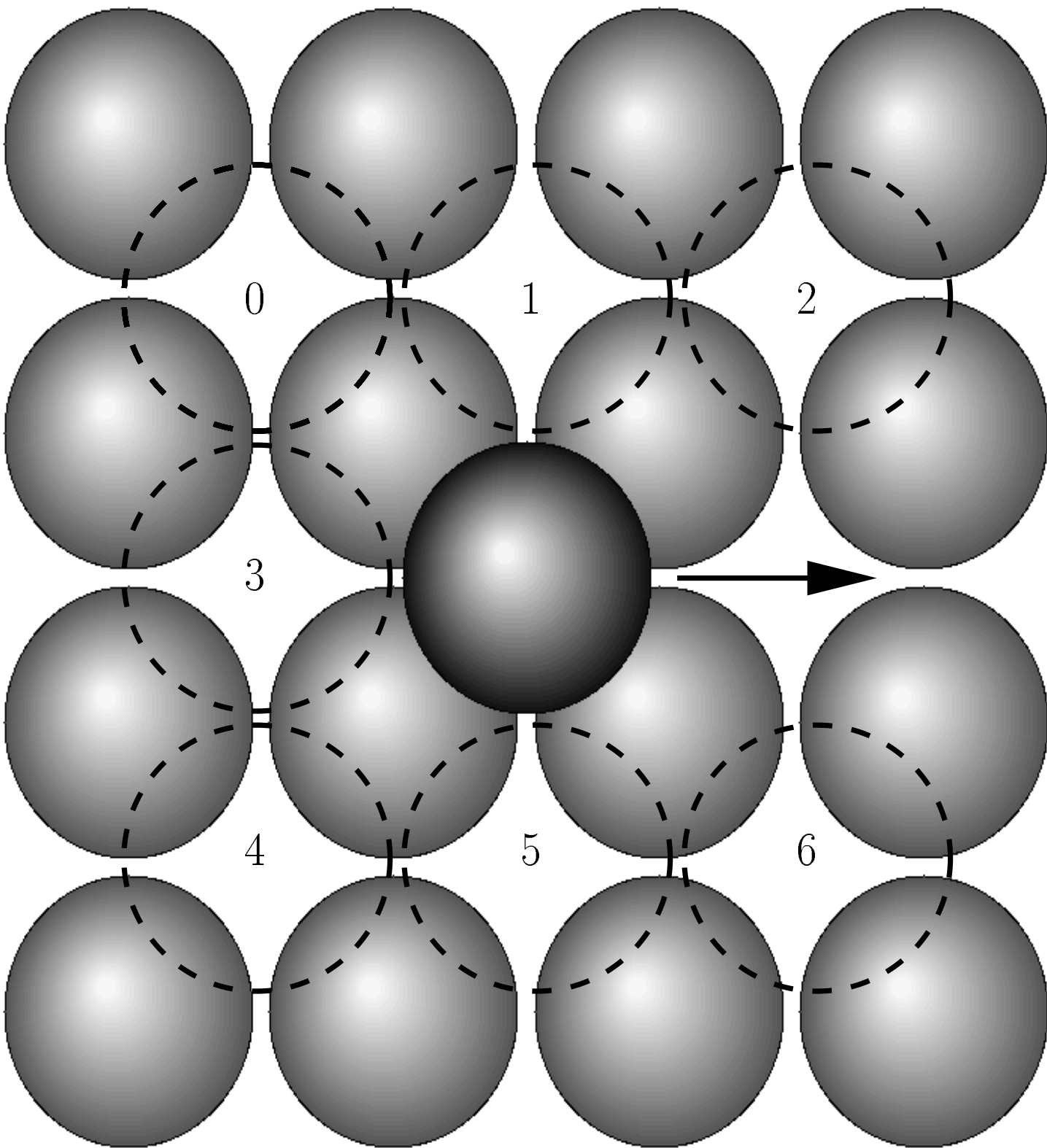


FIG. 1

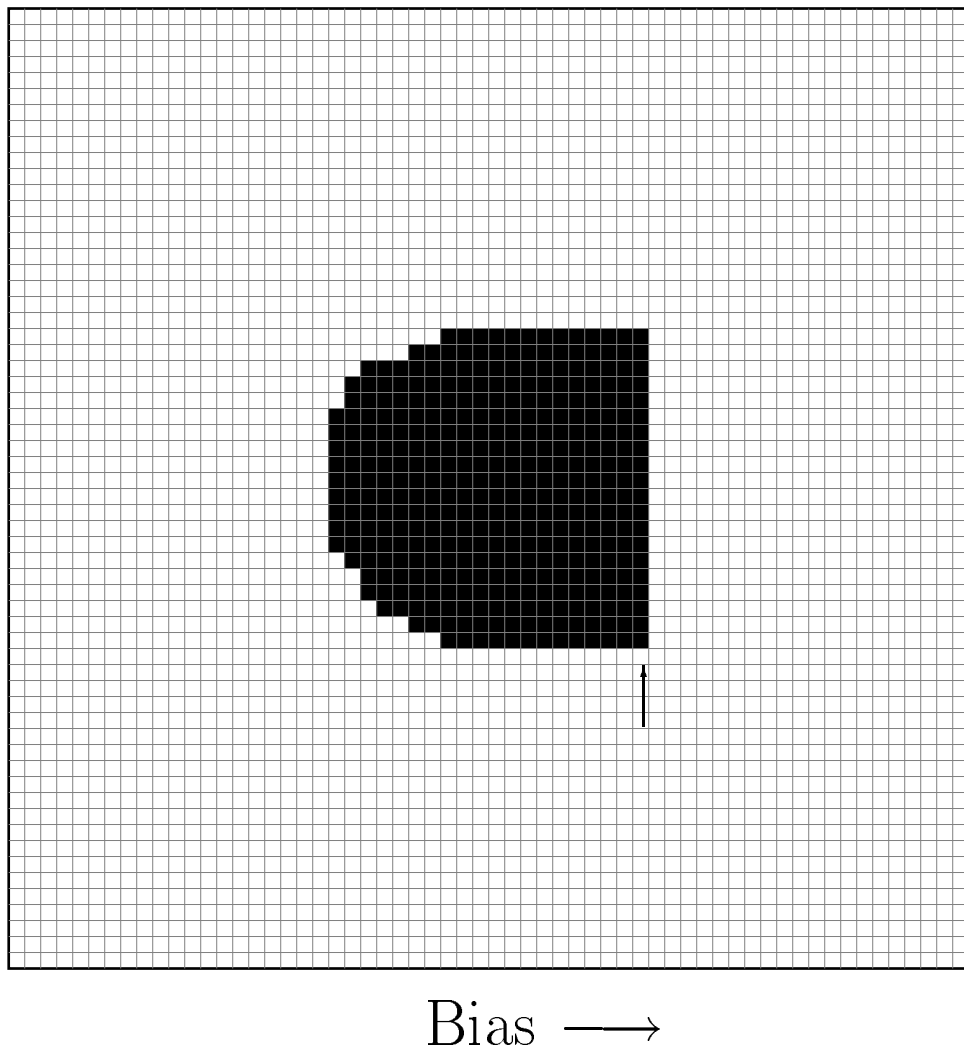


FIG. 2 (a)

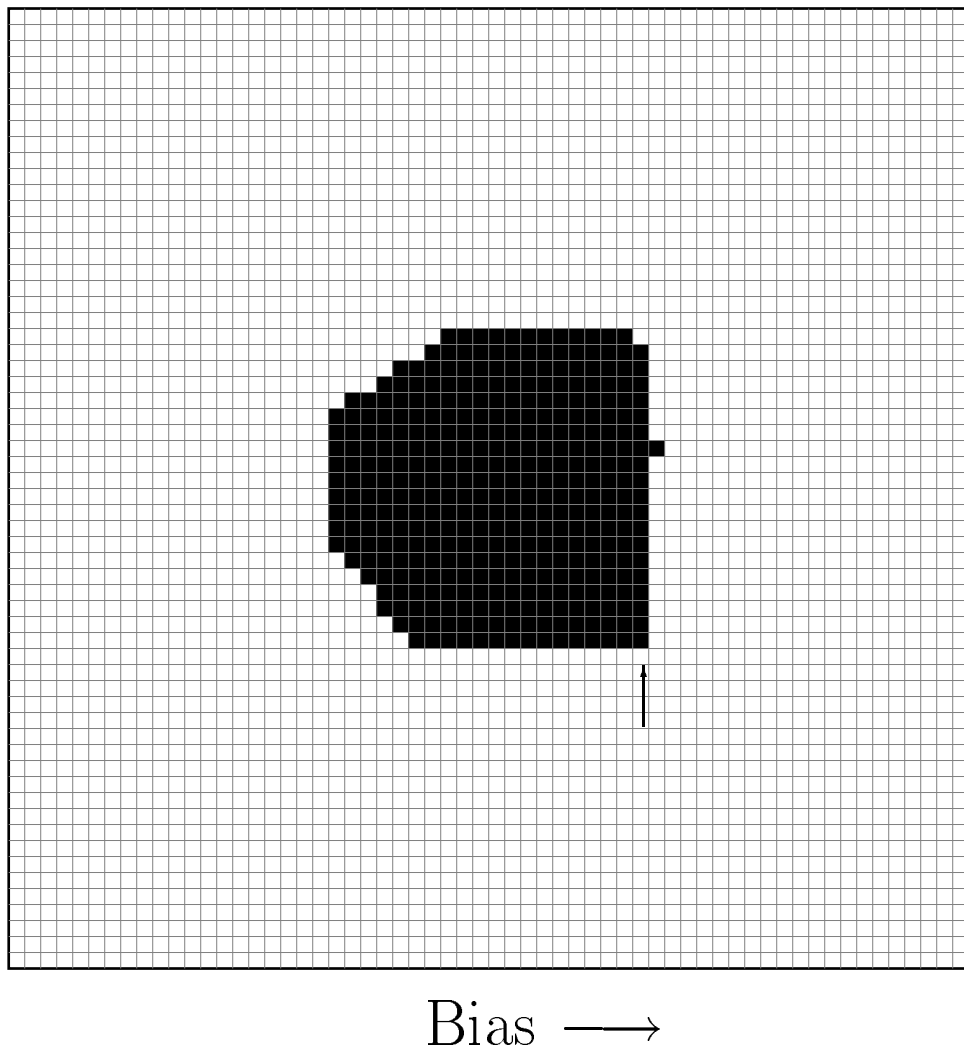


FIG. 2 (b)

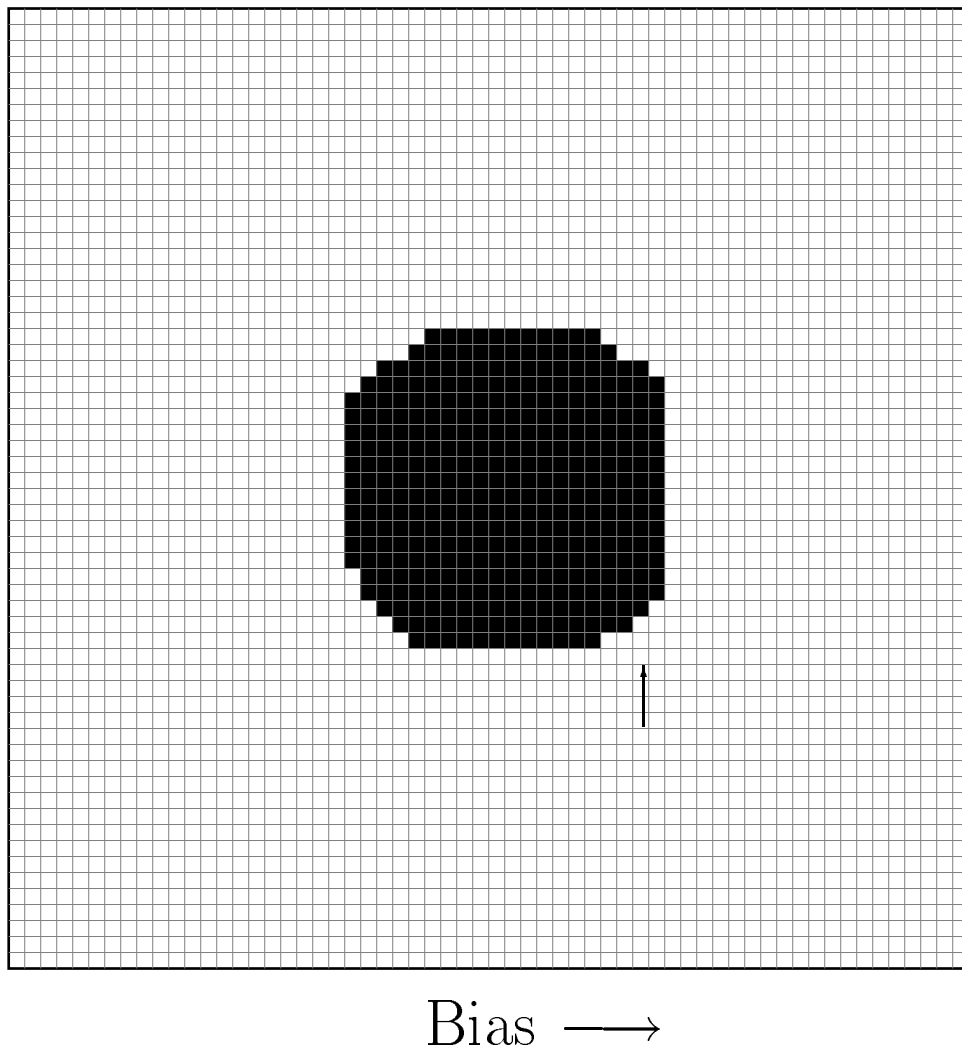


FIG. 2 (c)

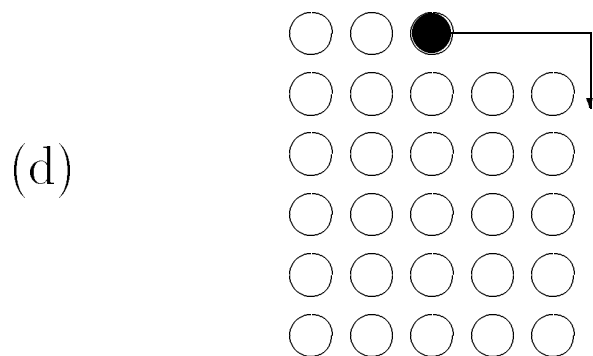
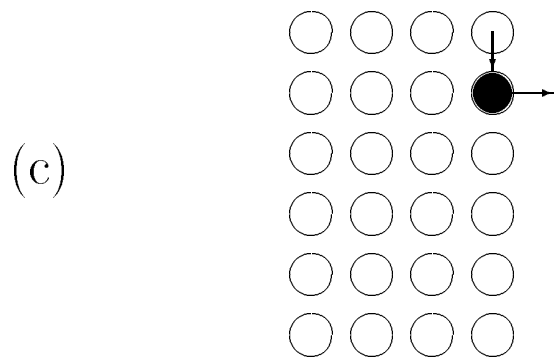
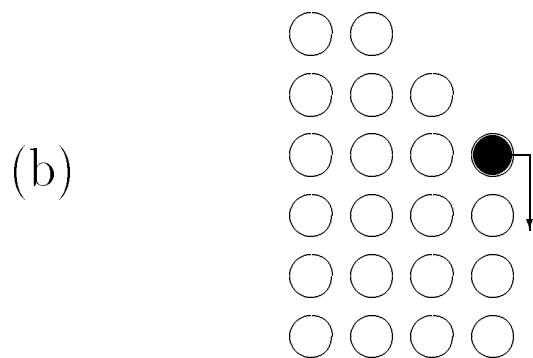
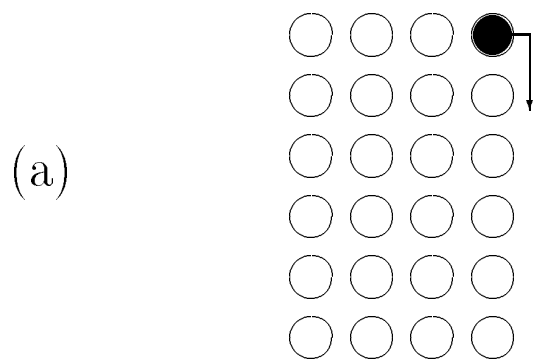


FIG. 3

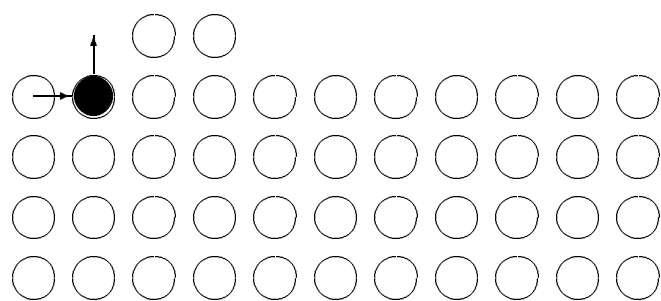
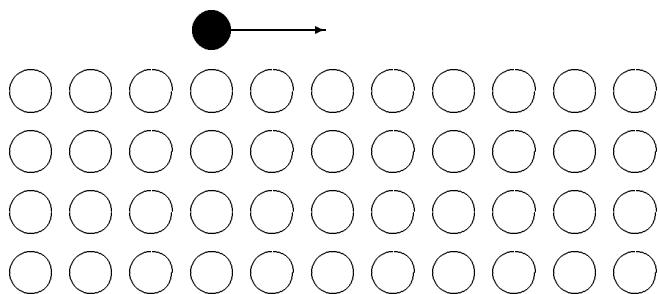
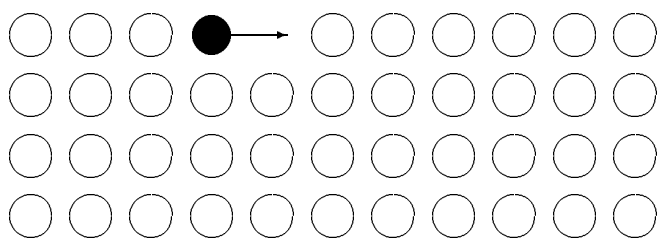


FIG. 4



Bias \longrightarrow

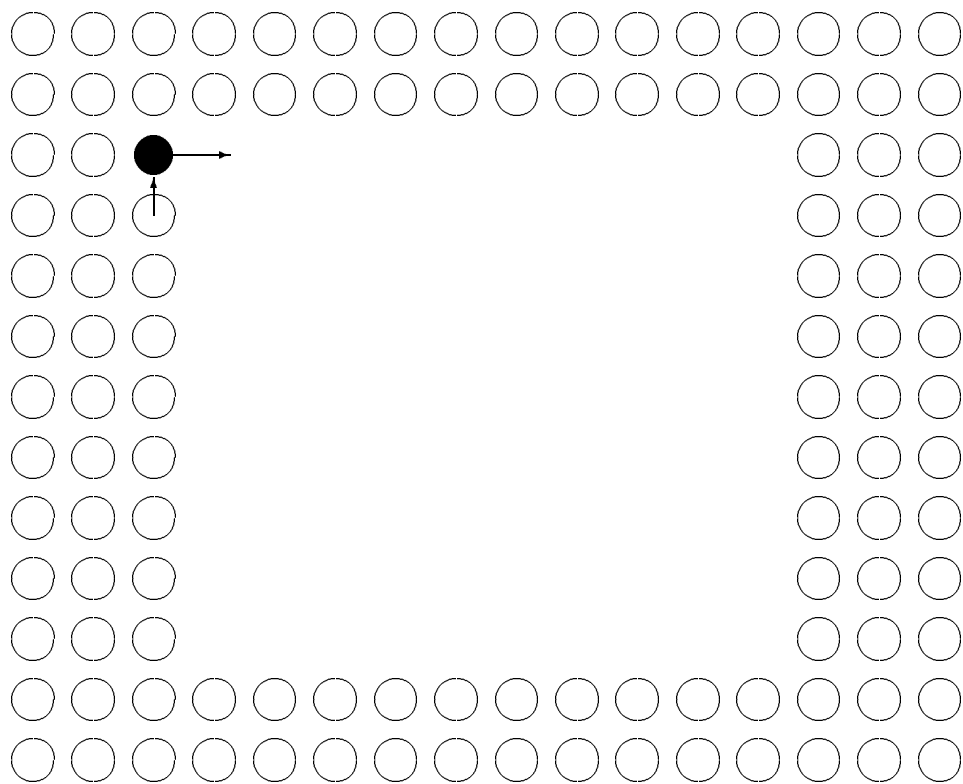
(a)



Bias \longrightarrow

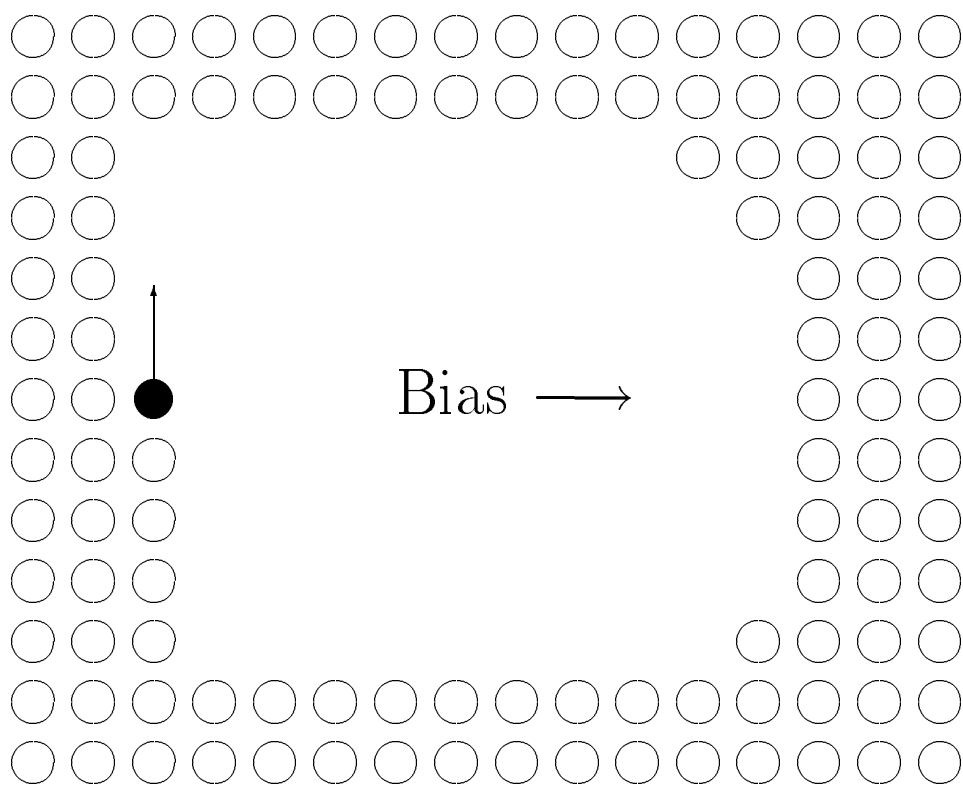
(b)

FIG. 5

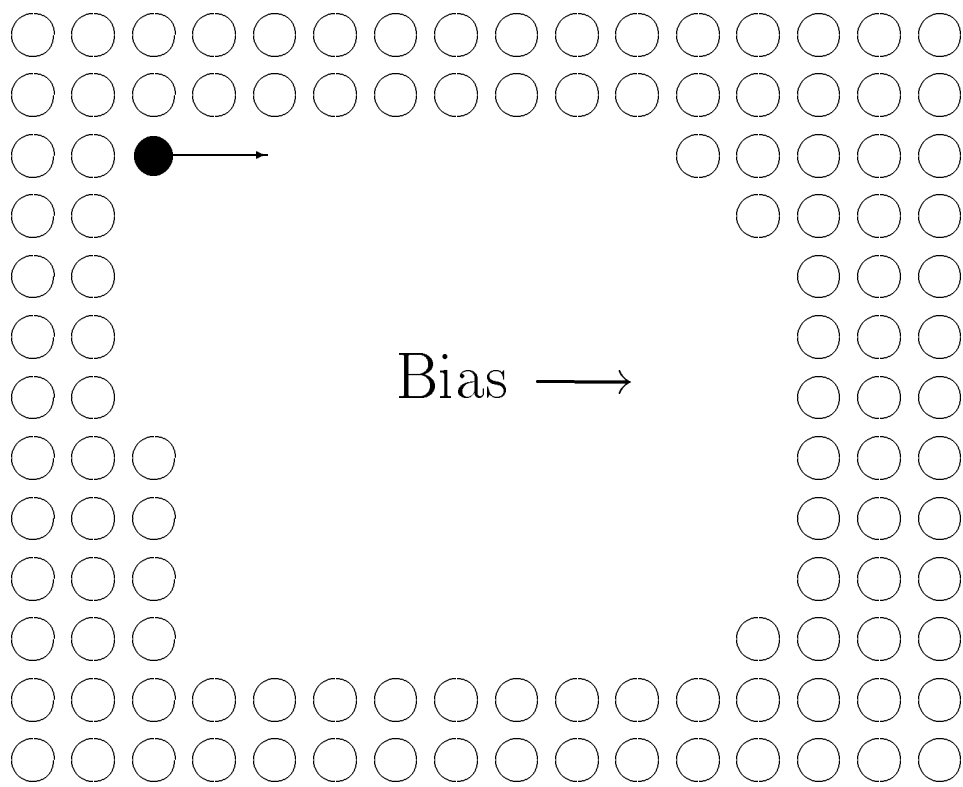


Bias \longrightarrow

FIG. 6



(a)



(b)

FIG. 7

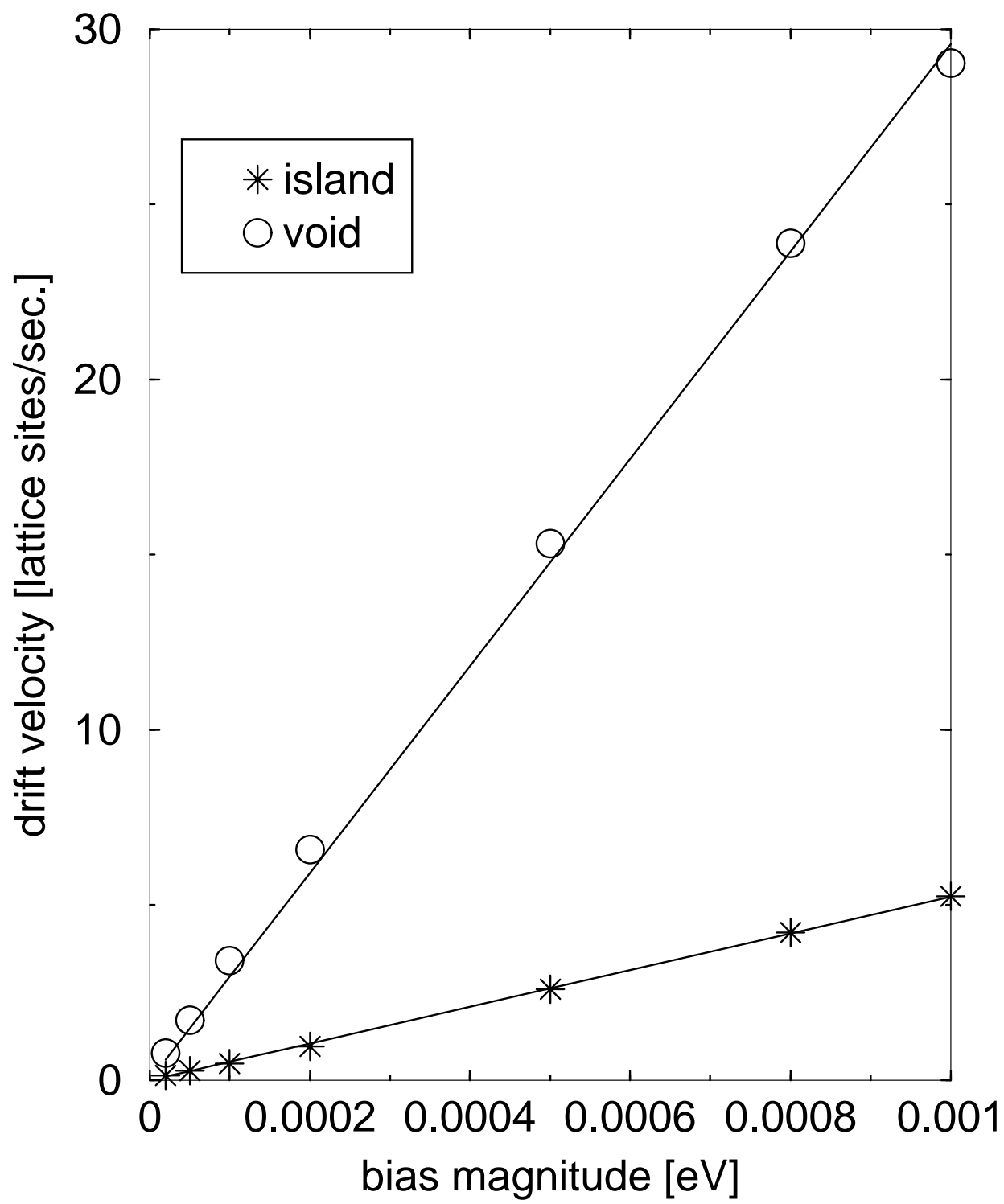


FIG. 8

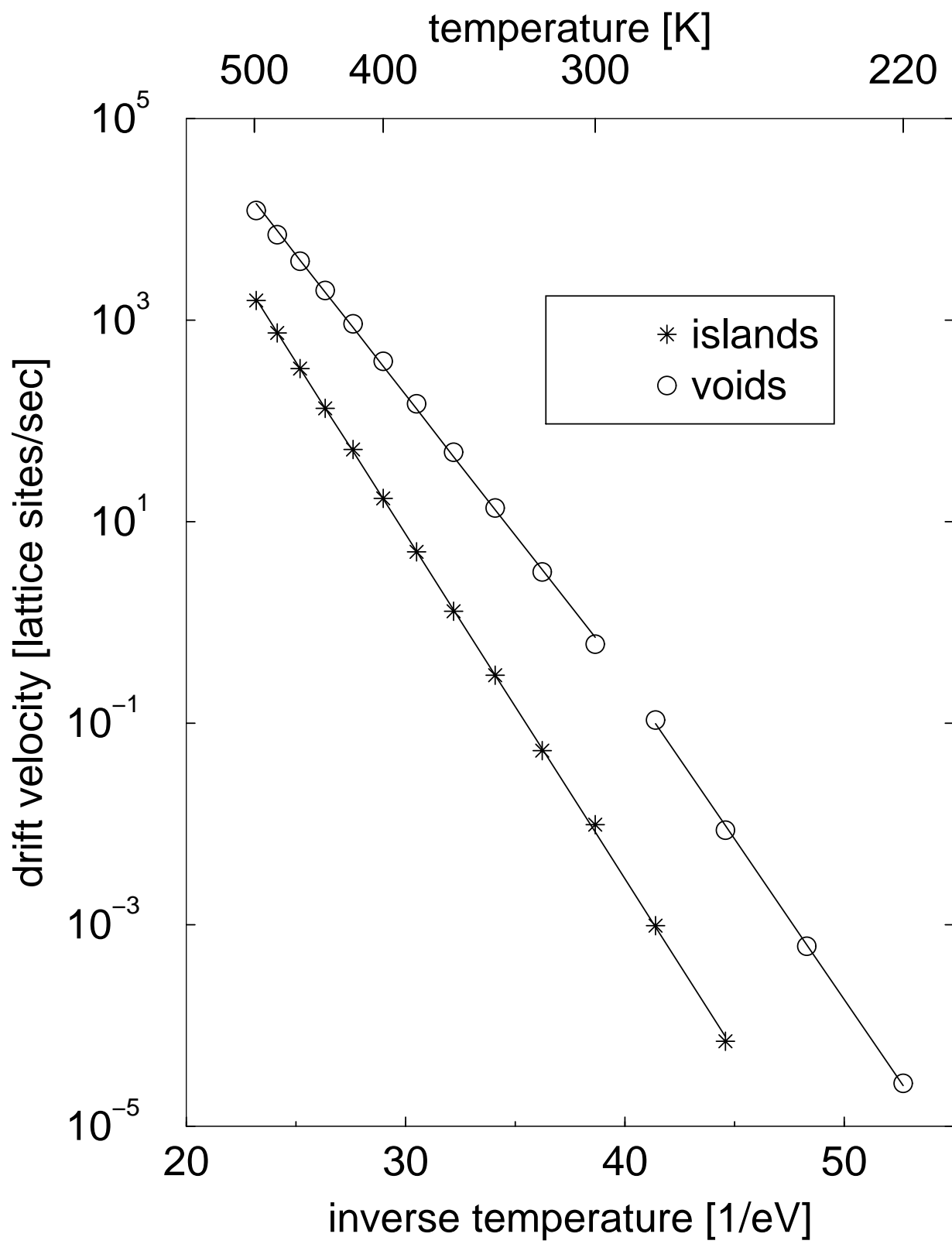


FIG. 9

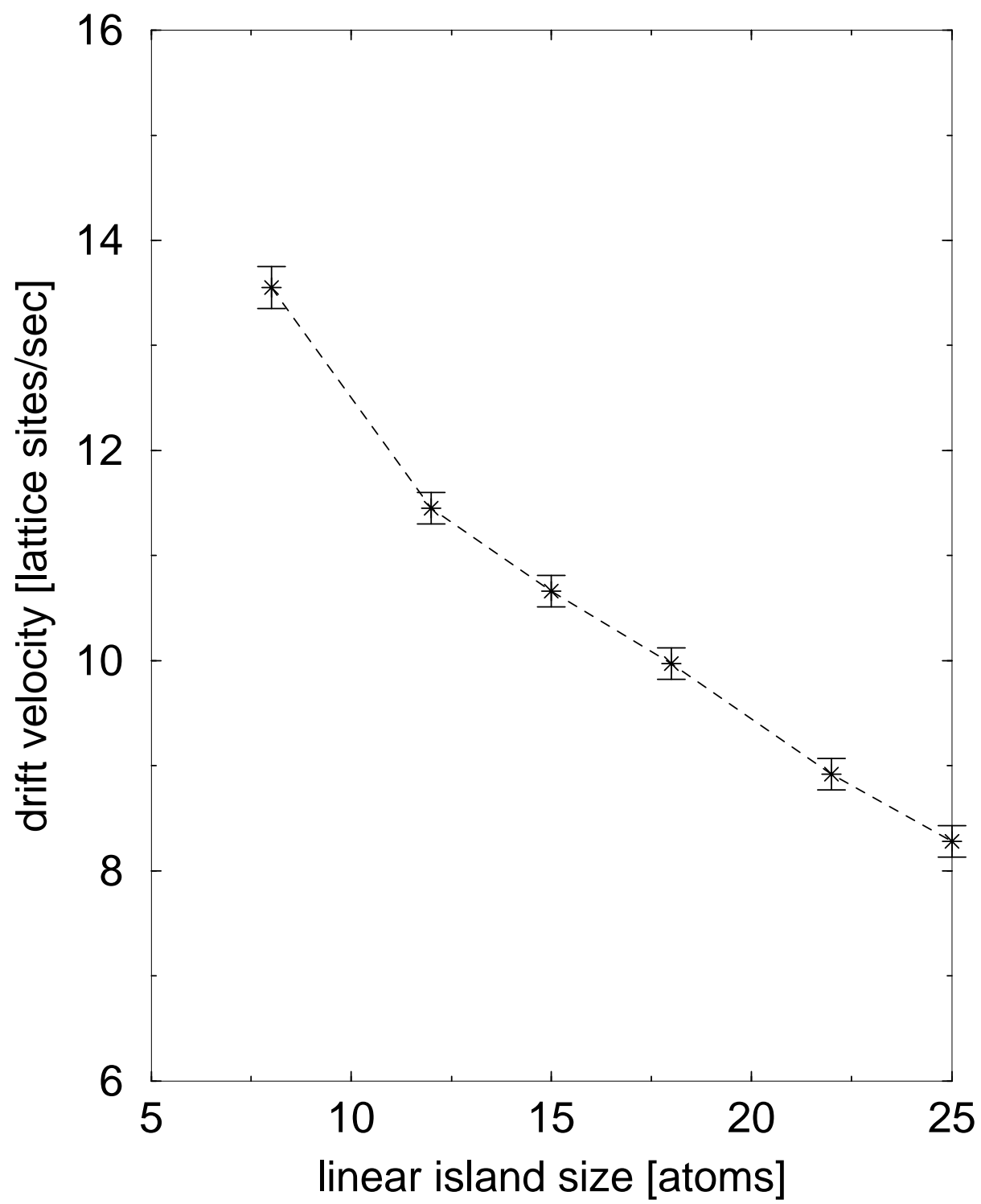


FIG. 10(a)

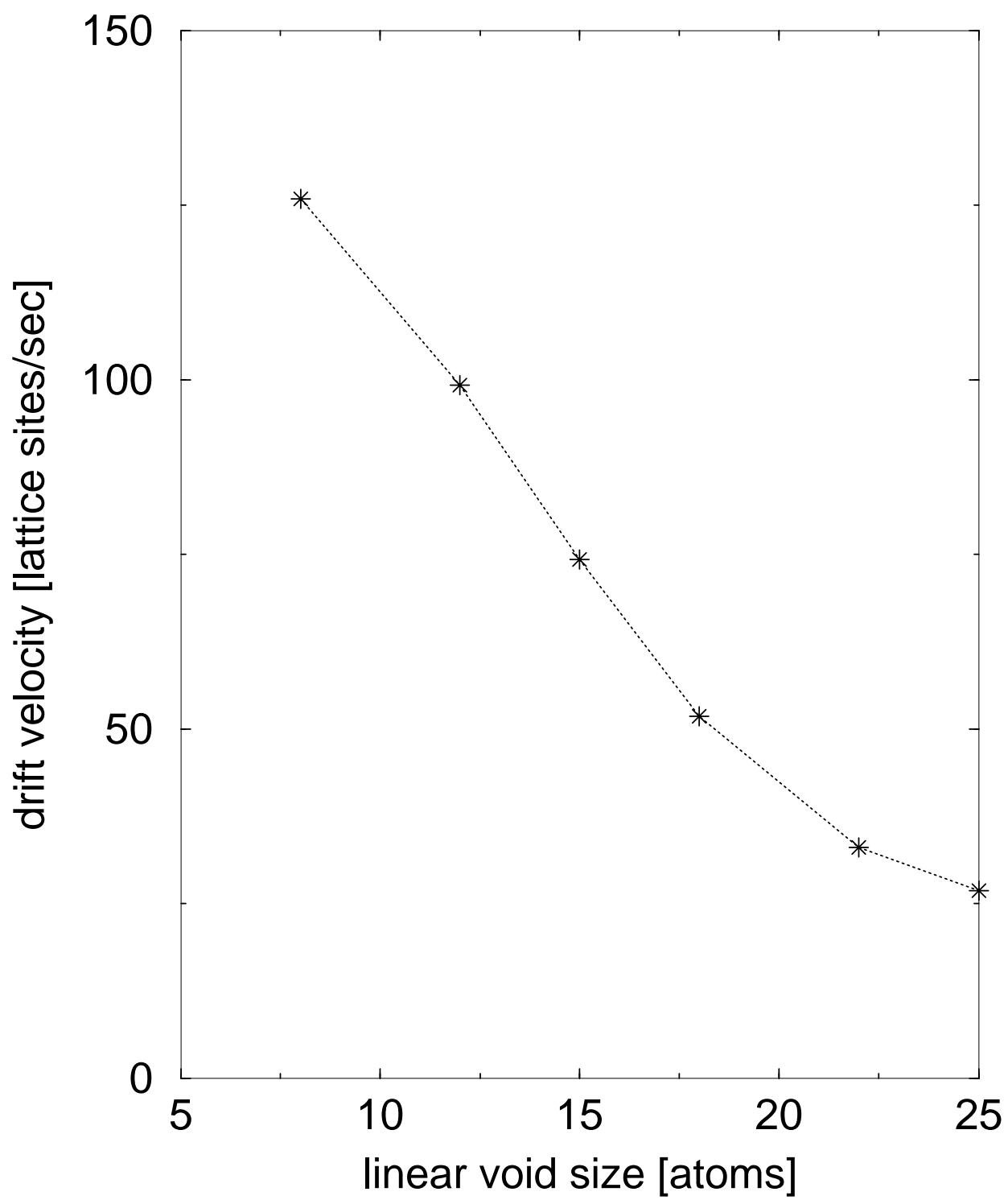


FIG. 10(b)